PERGAMON

Deep-Sea Research II 46 (1999) 279–303

DEEP-SEA RESEARCH
PART II

The mean flow field of the tropical Atlantic Ocean

Lothar Stramma*, Friedrich Schott

Institut für Meereskunde, an der Universität Kiel, Düsternbrooker Weg 20, 24105 Kiel, Germany

Received 26 August 1997; received in revised form 31 July 1998

Abstract

The mean horizontal flow field of the tropical Atlantic Ocean is described between 20°N and 20°S from observations and literature results for three layers of the upper ocean, Tropical Surface Water, Central Water, and Antarctic Intermediate Water. Compared to the subtropical gyres the tropical circulation shows several zonal current and countercurrent bands of smaller meridional and vertical extent. The wind-driven Ekman layer in the upper tens of meters of the ocean masks at some places the flow structure of the Tropical Surface Water layer as is the case for the Angola Gyre in the eastern tropical South Atlantic. Although there are regions with a strong seasonal cycle of the Tropical Surface Water circulation, such as the North Equatorial Countercurrent, large regions of the tropics do not show a significant seasonal cycle. In the Central Water layer below, the eastward North and South Equatorial undercurrents appear imbedded in the westward-flowing South Equatorial Current. The Antarcic Intermediate Water layer contains several zonal current bands south of 3°N, but only weak flow exists north of 3°N. The sparse available data suggest that the Equatorial Intermediate Current as well as the Southern and Northern Intermediate Countercurrents extend zonally across the entire equatorial basin. Due to the convergence of northern and southern water masses, the western tropical Atlantic north of the equator is an important site for the mixture of water masses, but more work is needed to better understand the role of the various zonal under- and countercurrents in cross-equatorial water mass transfer.

1. Introduction

Several research programs have been conducted in the tropical Atlantic in the past two decades. While the earlier programs like the GARP (Global Atmospheric Research Program) Atlantic Tropical Experiment (GATE) or the program Francais Océan Climat Atlantique Equatorial (FOCAL) mainly focussed on equatorial processes in the interior, the recent programs like the Western Tropical Atlantic

* Corresponding author. Fax: 0049 431 597 3821; e-mail: lstramma@ifm.uni-kiel.de.

0967-0645/99/$ – see front matter
PII: S0967-0645(98)00109-X

Experiment (WESTRAX) and the World Ocean Circulation Experiment (WOCE) had the large-scale circulation and the cross-equatorial water mass exchange as their central objectives.

The subtropical gyre of the South Atlantic Ocean reaches to depths of 500–1000 m (Peterson and Stramma, 1991), with decreasing velocities and a southward shift of the center of the suptropical gyre with depth, while the flow field of the tropical Atlantic shows several zonal currents and countercurrents that seem to be of smaller meridional and vertical extent. In this presentation the schematic mean horizontal flow field for the upper ocean of the tropical Atlantic is addressed, while related processes like equatorial upwelling and interannual to decadal variability are only briefly mentioned, eddies and wave processes are not discussed. The upper ocean circulation in the western equatorial Atlantic Ocean has recently been reviewed by Stramma and Schott (1996), and their findings regarding the western part will be included but the detailed description will not be reproduced.

As summarized by Schott et al. (1998), a vertical flow component is added to the horizontal flow field by the shallow South Atlantic tropical–subtropical cell (STC). The tropical–subtropical cell connects the subduction zones of the eastern subtropics of both hemispheres via equatorward boundary undercurrents with the Equatorial Undercurrent (EUC), and the return flow is through upwelling and poleward Ekman transport. In addition, a tropical cell is expected to exist in which part of the equatorial divergence is subducted at near-equatorial latitudes by Ekman convergence and returns to the EUC in the interior; but direct observational evidence for this cell is still missing. Due to the convergence of northern and southern water masses by equatorward boundary currents, the western tropical Atlantic north of the equator is an important site for the mixture of water masses from both hemispheres.

A description of the mean horizontal flow field from a combination of our own results (e.g., Schott et al., 1998) and from the literature will be presented for the water masses of the upper tropical Atlantic between 20°N and 20°S. Due to the limited space here, this description is not intended to be a complete review listing all major literature contributions, but only includes references on special regions or phenomena addressed.

2. The upper ocean water masses

Water mass exchange including net northward meridional heat transport across the equator is accomplished by warm Tropical Surface Water (TSW), Central Water, Antarctic Intermediate Water (AAIW) and upper Circumpolar Deep Water (uCDW) moving northward in the upper 1200 m compensated by cold North Atlantic Deep Water (NADW) moving southward between 1200 and 4000 m. At the bottom, the northward transport of Antarctic Bottom Water also carries a small amount of cold water into the northern hemisphere. The surface layer of the tropical Atlantic is occupied by the TSW. Underneath, two types of South Atlantic Central Water (SACW) are found, the lighter type originating from the southwestern subtropical South Atlantic and circulating in the subtropical gyre, while the denser type probably

originates from the southern South Atlantic as well as the South Indian Ocean and flows northward with the Benguela Current and then westward towards the tropical Atlantic with the South Equatorial Current (SEC).

The North Atlantic Central Water (NACW) can be distinguished from the SACW because it is saltier, warmer and contains less dissolved oxygen. Underneath the SACW, colder and fresher AAIW is found below about 500 m depth (Fig. 1). At about 1000 m depth, uCDW is the deepest water mass of the upper ocean, with a net northward transport.

The TSW with temperatures of about 27°C forms the mixed layer of the tropical Atlantic. In the sharp thermocline underneath, the temperature drops from 25°C to 15°C on about 50 m and the 20°C isotherm well represents the lower boundary of the TSW (Fig. 1a). Imbedded in the TSW is the Salinity Maximum Water (Defant, 1936), also called Subtropical Underwater (Lambert and Sturges, 1977), which is characterized by a salinity maximum at densities slightly below $\sigma_\Theta = 25.0$ at about 100 m depth. The Salinity Maximum Water is formed in the tropics/subtropics transition region by subduction (Tomzcak and Godfrey, 1993) and progresses equatorward as a subsurface salinity maximum (Fig. 1a), while the overlying water is salinity poor due to the high precipitation in the tropics. In the southern tropical Atlantic, subduction is active during August to October south of 12°S, coupled with the formation of a barrier layer (defined by the depth difference between the isothermal and isopycnal layer) to the north (Sprintall and Tomczak, 1992). On a meridional section at 25°W Tsuchiya et al. (1994) observed the highest surface salinities near 21°S. The subsurface salinity maximum in the western tropical Atlantic reaches values of 37.0 at 10 to 5°S, while staying below 36.7 north of the equator.

The Central Water masses are characterized by a nearly linear T–S relationship (Sverdrup et al., 1942). The SACW of the subtropical gyre is formed near the subtropical front in the southwestern South Atlantic. However, the SACW found in the tropical regions according to Sprintall and Tomczak (1993) and Tomczak and Godfrey (1994) is to a larger amount Indian Central Water brought into the Atlantic Ocean in modified form by Agulhas rings and filaments, enhancing in particular the volume of the water near 13°C. The associated thermostad can be traced from Namibia to the coast of Brazil near 10°S and into the eastward flowing components of the equatorial current system. Due to its thermostad and temperatures near 13°C, it is known as 13° – Water near the equator (Tsuchiya, 1986). The SACW covers the upper ocean of the subtropical South Atlantic and spreads northward underneath the TSW. A relative oxygen minimum at 300–500 m depth (Fig. 1b) is located at the lower part of the SACW in the tropics, which indicates a weak renewal in this region. This oxygen minimum is not a continuous layer but sometimes even consists of two minima. The SACW is transported within the SEC towards the Brazilian shelf, where it is carried towards the equator with the North Brazil Undercurrent (NBUC) and the North Brazil Current (NBC). The Central Water is slightly more saline north of the equator in the North Atlantic. The Cape Verde Frontal Zone (e.g. Siedler and Onken, 1996) corresponds to the boundary between NACW and SACW. This boundary extends zonally across the entire Atlantic (Lozier et al., 1995), from the Caribbean Sea

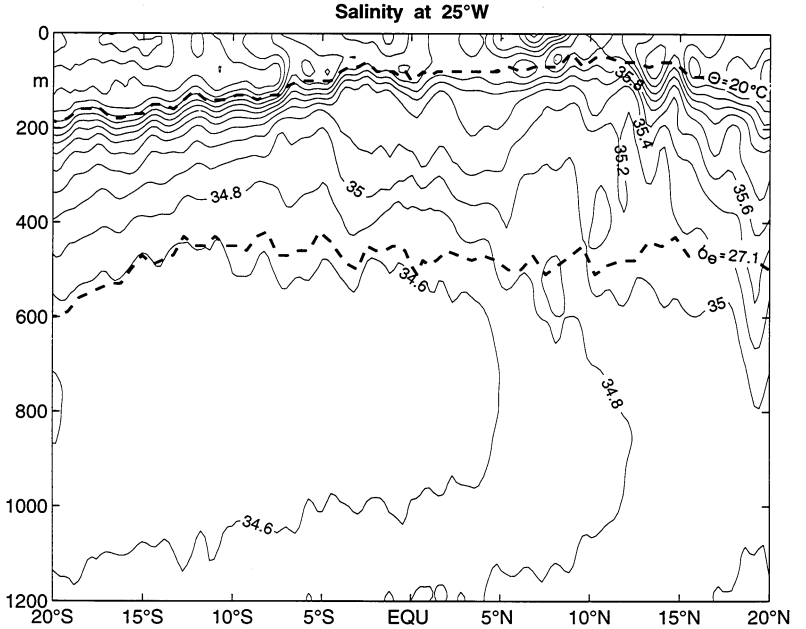
Salinity at 25°W
0
m
200
400
600
800
1000
1200
20°S
15°S
10°S
5°S
EQU
5°N
10°N
15°N
20°N
Θ=20°C
Θ=27.1
35.8
35.4
35.2
35.6
34.8
35
34.6

(a)

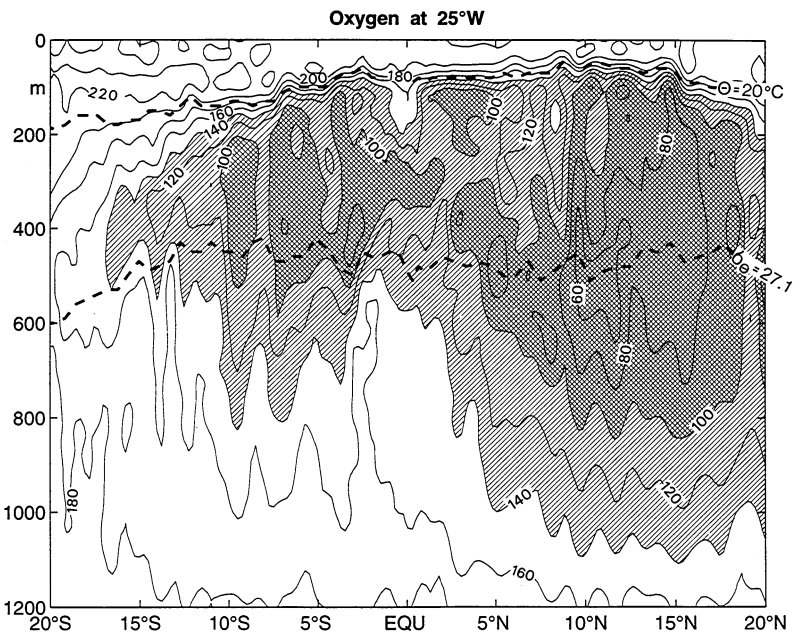
Oxygen at 25°W
0
m
200
400
600
800
1000
1200
20°S
15°S
10°S
5°S
EQU
5°N
10°N
15°N
20°N
Θ=20°C
Θ=27.1
220
200
180
160
140
120
100
80
60

(b)

along about 15°N, and takes on a more southwest–northeast orientation east of 30°W near the African shelf. The existence of this Central Water boundary was noted by Sverdrup et al. (1942), and a first detailed description of the eastern part of the boundary region was given by Tomczak (1984). With SACW and NACW occupying the same density range, the front is density-compensated and results in a multitude of intrusions, filaments and lenses (Tomczak and Godfrey, 1994). As the Central Water boundary is located at about 15°N, the equatorial Central Water circulation carries mainly SACW. In the eastern part of the Cape Verde Frontal Zone, Tomczak (1984) found an inclined boundary between NACW and SACW rising from south to north, i.e. SACW lying on top of NACW. Further west, the transition between these two water masses has a more vertical orientation. In the west the front looses largely its identity, as mixing in the North Equatorial Current (NEC) erodes the horizontal gradients.

The isopycnal $\sigma_\Theta = 27.1$ at about 500 m (Fig. 1a) marks the transition between the SACW and the AAIW. The AAIW in the South Atlantic originates from a surface region of the circumpolar layer, especially the surface waters in the northern Drake Passage and the Falkland Current loop and a southern boundary that is essentially the Subantarctic Front (Talley, 1996). It can be recognized by a subsurface oxygen maximum and a salinity minimum north of about 50°S, although the oxygen maximum becomes weak or absent in most areas north of 20°S in the open ocean, while it spreads along the Brazilian shelf equatorwards and eastward just south of the equator (Talley, 1996). A spreading of the AAIW identified by a salinity minimum near the equator at σ_Θ of about 27.3 (Tsuchiya, 1989) from the South Atlantic to the North Atlantic was described by Wüst (1935) who called this water Intermediate Water. The salinity minimum is present to 24°N (Reid, 1994), although traces of the AAIW can be followed as far north as nearly 60°N (Tsuchiya, 1989).

Below the AAIW, the northern limits of the uCDW occur near the equator, with phosphate and silica maxima and a temperature minimum at about 1000 m (Reid, 1989). This water has a source region different from the overlying AAIW, but both water masses flow from the South Atlantic towards the North Atlantic. The uCDW almost disappears near the equator, the vertical extent of this water mass is small, as are observed velocities and transports (Fu, 1981). Therefore, the uCDW flow field is included in the AAIW layer flow field. As can be seen from the zonal velocity distributions (Fig. 2), the equatorial currents are not completely confined to the different water masses, and the description of the flow field by water masses is only an approximation to separate the different vertical current distributions.

Fig. 1. The water masses on a meridional section along approximately 25°W from RV Oceanus in July to August 1988 north of the equator and RV Melville in February to April 1989 south of the equator (Tsuchiya et al., 1992, 1994) for (a) salinity and (b) oxygen in micromols per kilogram with light shading for oxygen less than 140 μmols/kg and strong shading for oxygen less than 100 μmols/kg. The water mass boundaries are shown by the 20°C isotherm and the density surface $\sigma_\Theta = 27.1$.

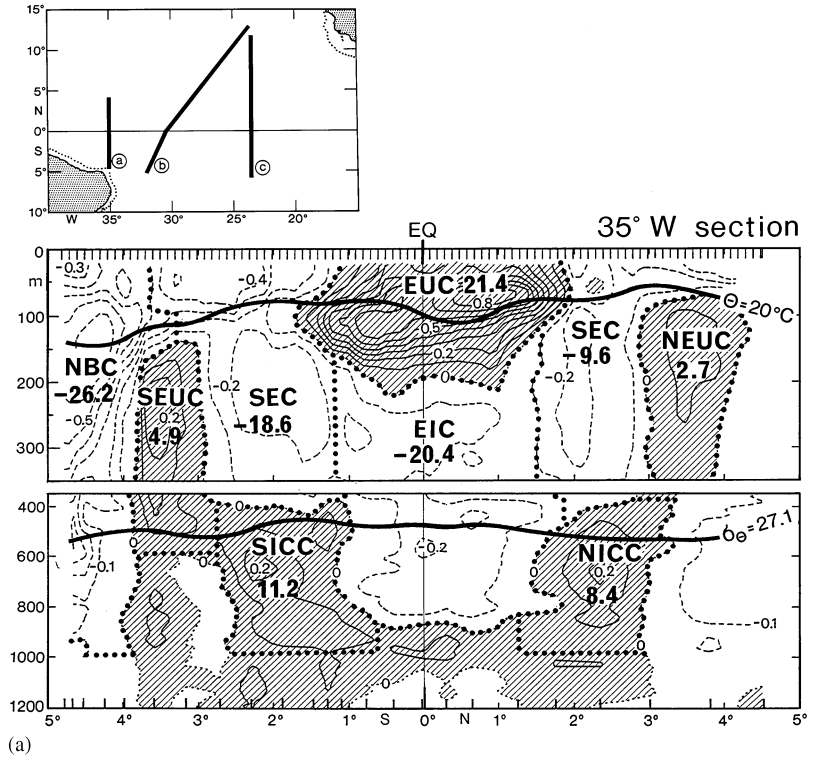
35° W section
EQ
EUC 21.4
Θ=20°C
NBC
-26.2
SEUC
4.9
SEC
-18.6
EIC
-20.4
SEC
-9.6
NEUC
2.7
SICC
11.2
NICC
8.4
σΘ=27.1
m
(a)
~30° W diagonal section
EQ
SEC
-14.7
EUC 15.4
Θ=20°C
SEC
-17.7
NECC
9.5
GD/NEC
-8.2
GD
6.6
SEUC
5.3
EIC
-5.8
NEUC
0.6
NICC
1.3
SICC
m
(b)

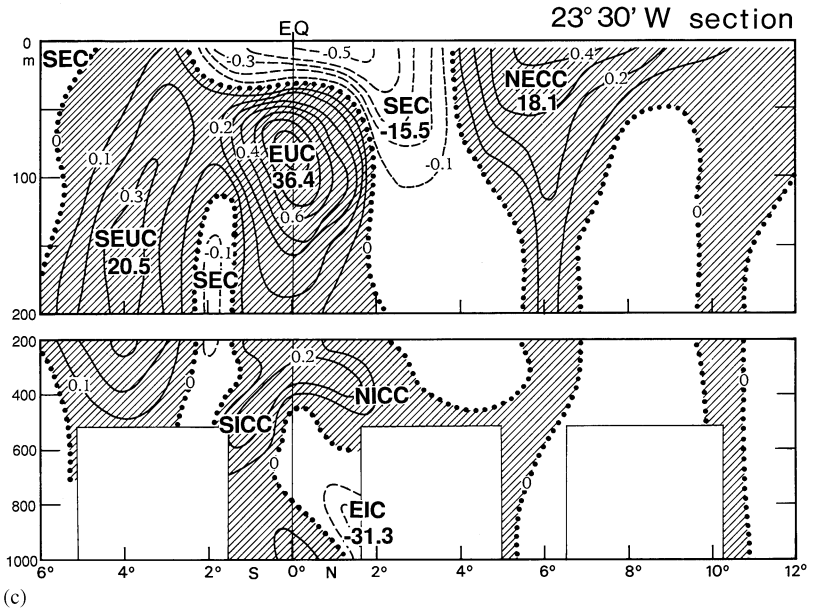

Fig. 2. Continued.

3. Air–sea interaction

The seasonal cycle is the largest atmosphere–ocean signal in the tropical Atlantic. The timing and characteristics of the seasonal evolution of the location of the Intertropical Convergenze Zone (ITCZ) and of the sea surface temperature depend on coupled dynamics and on land–sea contrasts in ways not yet fully understood.

The seasonal cycle of the surface currents (Fig. 3) reflects the response to the seasonally varying wind field and the migration of the ITCZ. With the ITCZ moving

Fig. 2. Zonal velocity components in m/s (eastward flow is shaded; see map for section location) for (a) from combined shipboard and lowered ADCP for the section at 35°W in March 1994 (after Schott et al., 1995), (b) from a diagonal section with shipboard ADCP at about 30°W in June 1991 and (c) from averages of moored current meter records and over-the-side current measurements from a research ship at 23°30′W averaged over June to September 1974 (after Bubnov and Egorikhin, 1980). Current branches are indicated and some transport numbers are given in Sv although with expected high uncertainties and unreliable transport numbers in 2c. Shown are the North Brazil Current (NBC), the South Equatorial Undercurrent (SEUC), the South Equatorial Current (SEC), the Southern Intermediate Countercurrent (SICC), the Equatorial Undercurrent (EUC), the Equatorial Intermediate Current (EIC), the Northern Intermediate Countercurrent (NICC), the North Equatorial Undercurrent (NEUC), the North Equatorial Countercurrent (NECC) the zonal components of the Guinea Dome (GD) and the North Equatorial Current (NEC). Also the water mass boundaries are shown by the 20°C isotherm and the density surface $\sigma_\Theta = 27.1$ in case accompanying CTD profiles were taken.

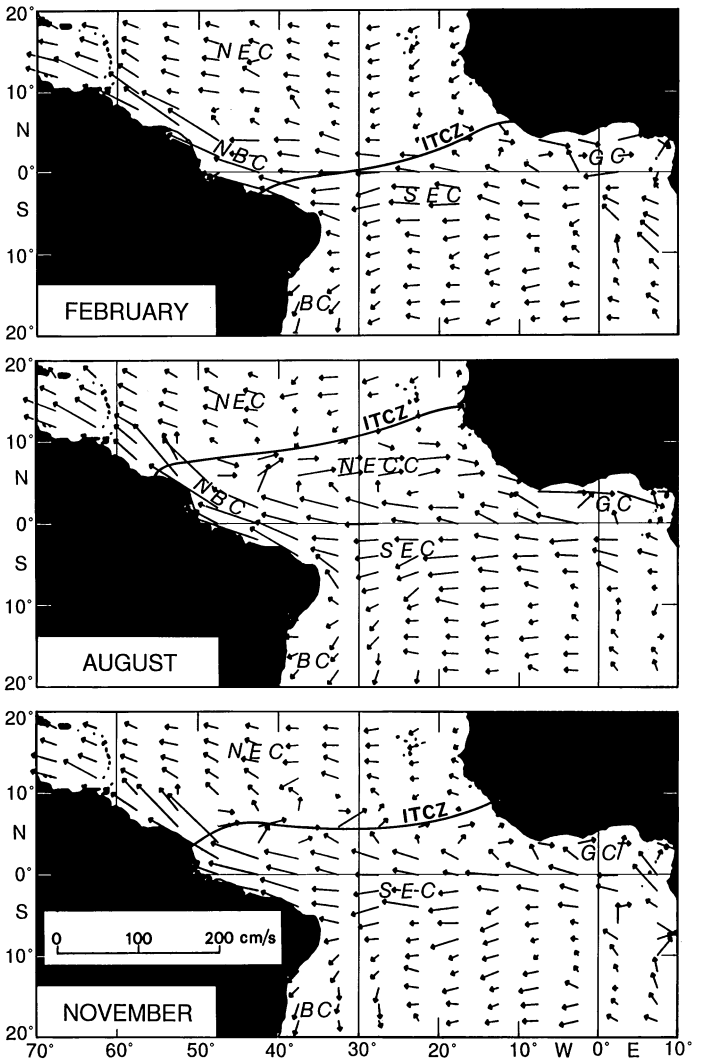

Fig. 3. Maps of shift drift velocity vectors for February, August and November, which illustrate the variation of surface currents throughout the year. Speed is proportional to the length of the tail of a vector (from Richardson and Walsh, 1986). The climatological position of the ITCZ (from Molinari et al., 1986) is included as solid line as well as the current bands for the North Equatorial Current (NEC), the South Equatorial Current (SEC), the North Equatorial Countercurrent (NECC), the North Brazil Current (NBC), the Brazil Current (BC) and the Guinea Current (GC).

northward from northern spring to summer, the zonal currents of the NEC and SEC also move northward. By late summer the southeast trade winds reach across the equator and the NBC retroflects eastward into the North Equatorial Countercurrent (NECC). However, the ship drift data (Fig. 3) are only valid for the shallow mixed

layer influenced largely by the wind, while the TSW underneath the Ekman layer may show different geostrophic flow characteristics in some regions such as the Angola Gyre in the eastern tropical South Atlantic, which is masked by the Ekman-layer flow.

In recent years, variability and deviations from the seasonal cycle were observed in the tropical atmosphere–ocean interface, and investigations and interpretation of these features have just begun. It is speculated that, superimposed on the mean seasonal cycle, two modes of ocean-atmosphere variability exist with significant impacts on the regional climate of the Americas and Africa. One of these presumed modes is the 'Tropical Atlantic Dipole' (e.g. Servain, 1991) characterized by a north–south interhemispheric gradient in sea surface temperature (SST). This mode involves spatially coherent SST variations in either hemisphere between about 5°N to 25°N and 5°N to 20°S, with dominantly decadal time scales. Interhemispheric SST anomalies significantly affect the position and intensity of the ITCZ and thus exert a considerable influence on the rainfall over the Nordeste and Sahel (e.g., Servain, 1991). When the SST north of the equator is positive, the ITCZ moves northward, leading to drought in northeastern Brazil and higher precipitation in the Sahel region. The analysis of about 100 yr of tropical sea surface temperatures showed an EOF-mode with a spectral maximum at 12–13 yr. Model studies result in a significant role of latent heat flux in these processes with a positive feedback between SST and heat flux. It is still controversial whether this dipole exists, since the dipole mode explains less than half the observed variance. Houghton and Tourre (1992) questioned the dipole character and suggested that the north- and south-hemispheric variations are uncorrelated.

A second mode of climate variability in the tropical Atlantic is similar to the El Nino/Southern Oscillation (ENSO) in the Pacific, with manifestations focussed primarily near the equator (Zebiak, 1993). This 'equatorial' mode, like the interhemispheric dipole mode, varies on seasonal and interannual time scales. During a warm ENSO phase, tradewinds in the western equatorial Atlantic are weak and SSTs near the equator are unusually high, especially in the eastern basin. During a cold phase, tradewinds in the western equatorial Atlantic are strong and SSTs near the equator are unusually low. Such variability will be investigated in the future within the context of the CLIVAR (climate variability and predictability) program and in the planned French/Brazilian/American program PIRATA (Pilot Research Moored Array in the Tropical Atlantic).

In a recent numerical simulation Huang and Shukla (1997) used a general circulation model of the tropical Atlantic forced with observed monthly surface wind stress for 1964–1987 and parameterized surface heat flux. The simulation produced interannual variations with timescales of two to three years. It was further found that the interannual variations are associated with tropical oceanic waves, stimulated by the fluctuations of the equatorial easterlies, which propagate eastward along the equator and westward to the north and south. The periods of these modes are determined by the meridional width of the equatorial wind anomaly. The decadel mode, however, is associated with the ocean's adjustment in response to a basinwide out-of-phase fluctuation between the northeast and southeast trade winds.

4. The tropical surface water layer

As the seasonal changes of the wind field lead to variations of the circulation in the tropical Atlantic, the schematic flow fields are presented in Fig. 4 for both the northern spring and northern fall. Most prominent is the well-known existence of the eastward-flowing NECC in northern fall with maximum velocities in August, when the ITCZ is located at the northernmost position (Fig. 3), while the NECC is weak or even reversing to westward flow in the western tropical Atlantic in northern spring. East of 25°W, the depth of the thermocline varies seasonally but its meridional tilt varies less and does not reverse; hence there is no reversal of the NECC. In June 1991, the NECC reached velocities of 60 cm s^{-1} at about 27°W (Fig. 2b). By contrast the thermocline in the west reverses its tilt seasonally, consequently leading to a reversal of the baroclinic geostrophic transport.

The seasonal changes of the southeastern North Atlantic subtropical gyre were investigated by Stramma and Siedler (1988). For the NEC they described a small northward shift of the NEC in the upper 200 m of about 3° north of the Cape Verde Islands in fall compared to spring (Fig. 4), probably related to the northward shift of the ITCZ, which also is seen in ship drift data (Fig. 3). However, the volume transport did not show significant seasonal changes.

Another seasonal signal is associated with the flow field and the related upwelling near the Northwest African coast. In northern winter and spring the wind field off the North African coast south of 20°N is southward, leading to a southward coastal current (the African Coastal Current) and local upwelling (Fig. 4). During summer and fall the southward wind near the coast diminishes and a northward flow along the coast exists (the Mauritania Current), supressing coastal upwelling (Mittelstaedt, 1983).

South of the Cape Verde Island a cyclonic circulation feature exists (Fig. 4), which is related to an upward displacement of isotherms within the Guinea Dome (Mazeika, 1967). Siedler et al. (1992) showed that the dome and the related circulation exist throughout the year, but weaken in winter. Seasonal changes occur with respect to the vertical structure, horizontal extent and position of the Guinea Dome. The upper thermocline center of the dome is found at 9°N, 25°W in summer and at 10.5°N, 22°W in winter (Siedler et al., 1992). In June 1991 the reversal in flow direction in this region was observed at about 10°N (Fig. 2b).

Fig. 4. Schematic map showing the horizontal distribution of the major tropical currents for the Tropical Surface Water layer at about 0–100 m depth for (a) northern spring and (b) northern fall. Shown are the North Equatorial Current (NEC), the Guinea Dome (GD), the North Equatorial Countercurrent (NECC), the Guinea Current (GC), the South Equatorial Current (SEC) with the northern (nSEC), equatorial (eSEC), central (cSEC) and southern (sSEC) branches, the Equatorial Undercurrent (EUC), the North Brazil Current (NBC), the Gabon-Congo Undercurrent (GCUC), the Angola Gyre (AG), the Angola Current (AC), the Angola Dome (AD), the South Equatorial Countercurrent (SECC) and the Brazil Current (BC). The Angola-Benguela Front (ABF) is included as a dashed line. The symbol u in a square marks possible areas of upwelling, but not the exact places.

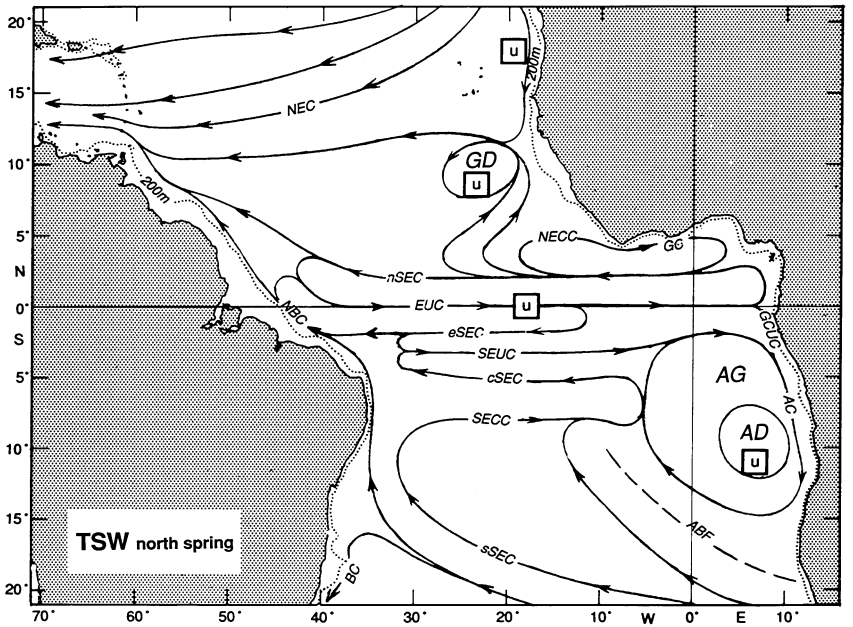
NEC
GD
u
200m
NECC
GC
nSEC
EUC
NBC
eSEC
SEUC
cSEC
SECC
AG
AD
AC
ABF
sSEC
BC
TSW north spring
20°
15°
10°
5°
N
0°
S
5°
10°
15°
20°
70°
60°
50°
40°
30°
20°
10°
W
0°
E
10°

(a)

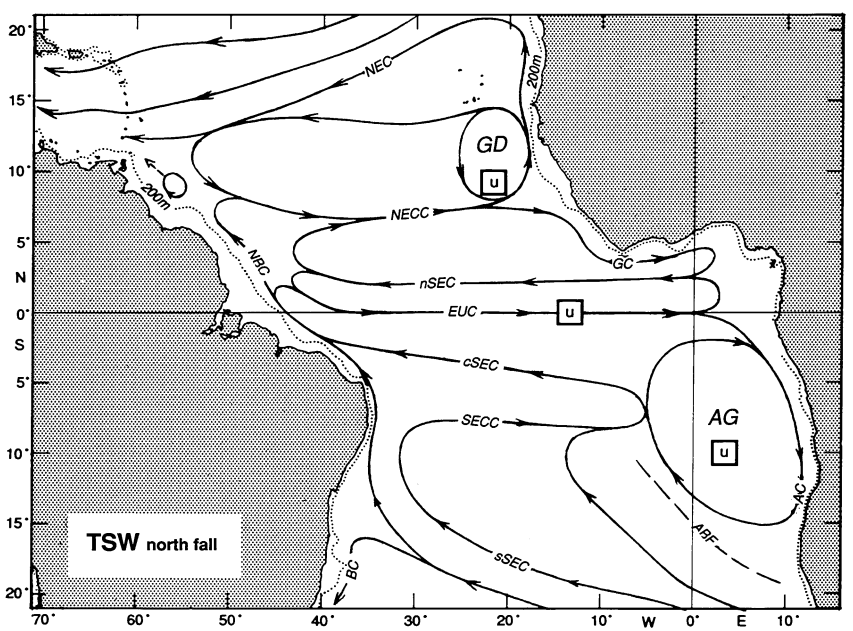
NEC
GD
u
200m
NECC
GC
NBC
nSEC
EUC
cSEC
SECC
AG
AC
ABF
sSEC
BC
TSW north fall
20°
15°
10°
5°
N
0°
S
5°
10°
15°
20°
70°
60°
50°
40°
30°
20°
10°
W
0°
E
10°

(b)

In the Gulf of Guinea, the coastal Guinea Current transports low-salinity, warm waters eastward from its western Atlantic origin, as an extension of the NECC (Hisard and Merle, 1980). The other important surface flow in the Gulf of Guinea is the SEC, which is separated from the Guinea Current by the northern tropical convergence along 3°N. At the equator, the thickness of the SEC sharply decreases due to the presence of the EUC.

The counterpart to the Guinea Dome in the southern hemisphere is the Angola Dome (Mazeika, 1967). As reviewed by Peterson and Stramma (1991) the Angola Dome is seen in the upper-layer temperature distribution during southern summer, but not winter. It is centered at 10°S, 9°E and, according to Voituriez (1981), is different from the larger-scale Angola Gyre, imbedded itself below the TSW layer in a basin-wide tropical cyclonic gyre also called cyclonic subequatorial gyre (Tsuchiya et al., 1994; Suga and Talley, 1995). The Angola Dome in the thermocline corresponds to a seasonal uplifting of the deeper structure when low atmospheric pressure and favorable wind stress curl cause upwelling, hence by the local wind field, while the Angola Gyre is formed by the large-scale current field. The Angola Gyre is centered near 13°S, 5°E (Gordon and Bosley, 1991), its eastern side being formed by the southward-flowing Angola Current. The confluence of the Angola Current with the cold northward-flowing Benguela Current causes a sharp thermal front, the Angola–Benguela Front, which is well developed in the upper 50 m and detectable in the salinity field to depths of at least 200 m.

Molinari (1982) described the SEC as divided into three bands in the South Atlantic, separated by the South Equatorial Undercurrent (SEUC) and the South Equatorial Countercurrent (SECC), respectively. The flow north of the SEUC was called northern SEC (nSEC), the flow between the SEUC and the SECC central SEC (cSEC) and the flow south of the SECC southern SEC (sSEC). As the nSEC is further separated by the EUC, we will refer to flow between the EUC and the SEUC as the equatorial SEC (eSEC) and only north of the equator as the nSEC. Stramma (1991) described the sSEC as a broad and sluggish flow between 10°S and 25°S east of 30°W. Only the southern part of the sSEC turns south into the Brazil Current when reaching the Brazilian shelf between 10°S and 20°S, and direct observations (Evans and Signorini, 1985) show the existence of the Brazil Current south of 20°S.

The inflow of the sSEC into the western equatorial regime was described by Stramma and Schott (1996). The sSEC at 12–20°S feeds into the the NBUC (mainly in the Central Water layer). It supplies the eastward flow of the SECC, which in turn partially recirculates in the cSEC. Off Brazil, the cSEC forms the surface-intensified NBC west of 35°W and then crosses the equator northwestward. These currents show only a weak seasonal signal (Schott et al., 1998).

As regards the eastern tropical South Atlantic, not much is known about the water exchange and interaction between the Angola Gyre and the SECC. The SEUC reaches the surface layer somewhere east of 35°W as an eastward flow during northern spring (Fig. 4a). From observations between 25°W and 28°W Molinari (1982) described the surface flow above the SEUC as being to the east during northern winter and to the west during July to August. Current observations at 5°W in January and

July 1975 (Hisard et al., 1976) also show strong westward flow above the SEUC in July and weak westward flow in the upper 40 m and eastward flow below in January.

The large Ekman flow divergence in the equatorial Atlantic of about 25 Sv between 8°N and 8°S (e.g., Roemmich, 1983) is compensated by upwelling on the order of 12 Sv (Gouriou and Reverdin, 1992) and geostrophic convergence in the near-surface layer in the equatorial region. The equatorial upwelling leads to a transfer of Central Water from the South Atlantic to the near surface layer where it continues to the northern hemisphere after taking up heat from the atmosphere in the equatorial zone (Roemmich, 1983). Besides equatorial upwelling the cyclonic gyres in the eastern tropical North and South Atlantic and African coastal upwelling are potential regions to bring deeper water masses towards the surface (Fig. 4). As even less is known from observations on downwelling sites, no symbols for downwelling are included in the schematic flow-field figures.

In the equatorial Atlantic west of 44°W, a large fraction of the NBC retroflects and feeds the EUC located in the lower part of the TSW and in the upper part of the Central Water (Figs. 4 and 5). In the western central equatorial Atlantic, the EUC transport estimates do not show a well-defined seasonal cycle, although somewhat lower values have been described for April–July than for October–February (e.g. Stramma and Schott, 1996). The EUC crosses the entire Atlantic while reducing in strength. Part of the EUC upwells in the equatorial region. Direct budgets, although with a high uncertainty, yield an estimate of 11–12 Sv upwelling (Gouriou and Reverdin, 1992), while an inverse calculation, including bomb radiocarbon distributions, result in upwelling rates between 7 and 10 Sv (Wunsch, 1984). Equatorial upwelling is indicated in Fig. 4 by a square around an u, this symbol representing the general equatorial upwelling and not the exact place where upwelling takes place. It is not known how much water of the EUC turns north into the nSEC and how much turns south into the eSEC.

At the eastern side of the tropical Atlantic a large fraction of the EUC seems to turn southward into the Gabon-Congo Undercurrent (GCUC) along the African coast at 1–6°S (Wacongne and Piton, 1992). This undercurrent is marked for the surface layer in Fig. 4a since in northern spring and summer the GCUC was observed already below 20 m depth in northern spring and fall. Along the Gabon and Congo coasts a thin surface current flows to the north, but the main transport is southward due to the GCUC.

In the eastern tropical Atlantic one might expect a seasonal variation of the EUC, because the easterly component of the wind stress (responsible for setting up the eastward zonal pressure gradient force believed to drive the EUC) goes through a distinct seasonal cycle with a maximum between May and November. Yet, equatorial current meter moorings at 28°W and 4°W do not show significant changes in the EUC transport, but rather a seasonal variation in the depth of the maximum eastward flow (Wacongne and Piton, 1992). In any event, only an indirect relation is to be expected between the EUC and the wind stress, because the establishment of a zonal pressure gradient and the time scale of it depends on the scale of the basin and the travel times of equatorial Kelvin and Rossby waves (e.g., Cane, 1979).

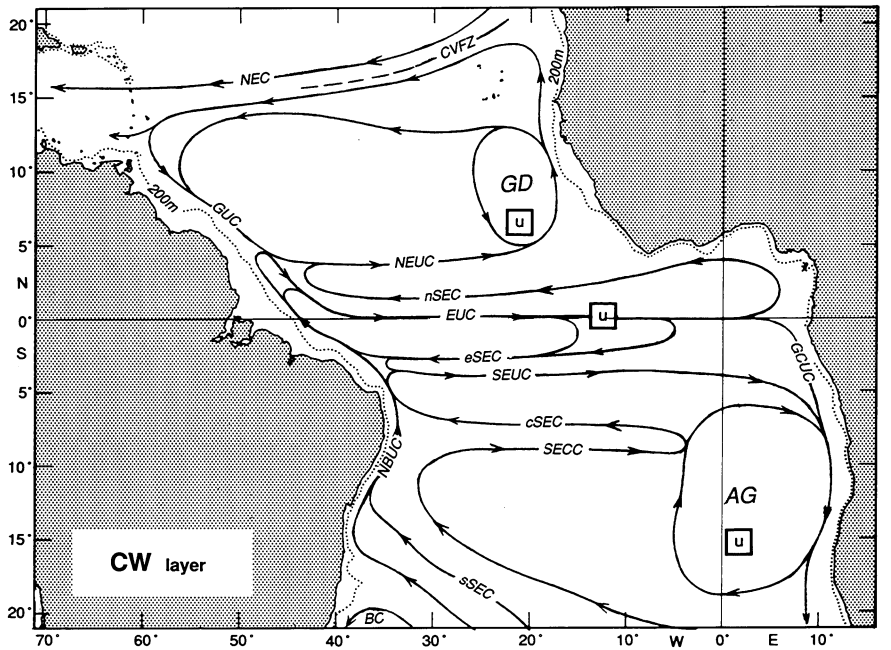

Fig. 5. Schematic map showing the horizontal distribution of the major tropical currents for the Central Water layer at about 100–500 m depth. Shown are the North Equatorial Current (NEC), the Guinea Dome (GD), the North Equatorial Undercurrent (NEUC), the Guiana Undercurrent (GUC), the South Equatorial Current (SEC) with the northern (nSEC), equatorial (eSEC), central (cSEC) and southern (sSEC) branches, the Equatorial Undercurrent (EUC), the North Brazil Undercurrent (NBUC), the Gabon-Congo Undercurrent (GCUC), the Angola Gyre (AG), the South Equatorial Undercurrent (SEUC), the South Equatorial Countercurrent (SECC) and the Brazil Current (BC). The Cape Verde Frontal Zone (CVFZ) is included as a dashed line. The symbol u in a square marks possible areas of upwelling, but not the exact places.

Based on observations and model results for the eastern Atlantic, Wacongne and Piton (1992) suggest a seasonally terminating EUC. In northern spring and summer (Fig. 4a) it would spread inertially along the equator, reach the eastern boundary, replenish the salt reservoir and create a deep poleward zonal pressure gradient force resulting in a well-defined salty southeastward GCUC; at other times it would partly branch off the equator before 1°E, yielding an eastward flow in the latitude range 2–8°S that may in turn reach the coast and feed the GCUC near 4–6°S (Fig. 4b).

In boreal spring part of the TSW of the NBC retroflects into the EUC, while part of the NBC continuous its northwestward flow resulting in water from the tropical Atlantic reaching the northwestern part of the South American continent. The northwestward flow along the South American coast is the Guiana Current. Schott et al. (1998) reported a northwestward alongshore throughflow of about 10 Sv ($1\ \mathrm{Sv} = 10^6\ \mathrm{m^3\ s^{-1}}$) of waters from the southern hemisphere along the Guiana boundary. In boreal fall, part of the NBC flows along the South American coast and feeds

the NECC through a retroflection, merging with water from the NEC. From observations in August 1989, Wilson et al. (1994) estimated that the NECC is composed of 16 Sv of NBC transport retroflected from the coast between 6°N and 8°N and 8 Sv supplied out of the NEC. No continuous throughflow of the NBC to the Caribbean was observed in that survey. At 25°W Tsuchiya et al. (1992) observed high salinities in the NECC, which do not exist in the North Atlantic north of the NECC, and they concluded that a significant amount of South Atlantic water is carried in the NECC. At the retroflection of the NBC into the NECC at about 10°N, anticyclonic eddies detach from the NBC (Fig. 4b) and move towards the Caribbean (e.g. Didden and Schott, 1993). The eddy generation season is the late retroflection phase, between October and February, and eddy shedding is an important phenomenon for the cross-equatorial water exchange.

A review on the throughflow from the tropical North Atlantic to the Caribbean was given by Schott and Molinari (1996). According to Schmitz and Richardson (1991) the flow from the Caribbean through the Straits of Florida for temperatures greater than 24°C is primarily composed of waters from the southern hemisphere that enter the Caribbean along the South American coast or in northern fall via the NECC, and in retroflection eddies moving northwestward off the South American continent. This agrees with direct observations of inflow of South Atlantic water into the Caribbean in the major southern Passages (Wilson and Johns, 1997) although they measured much smaller transport rates.

5. The central water layer

The mean flow field of the upper part of the Central Water layer based on the results given below is shown in Fig. 5. As described at the beginning of this paper, the Cape Verde Frontal Zone at about 15°N separates the NACW and SACW, and hence the tropical Central Water circulation carries mainly SACW. According to Schmitz and Richardson (1991) the middle layer (12–24°C) of the flow from the Caribbean through to the Straits of Florida is almost completely NACW. The water mass origin is controversial, as other investigations indicate a transfer of SACW into the Caribbean mainly in the upper part of this layer (e.g., as indicated by the stream function from an edited set of the historical hydrographic data of the North Atlantic on the density $\sigma_\Theta = 26.5$ relative to a density surface near 2000 dbar shown by Lozier et al., 1995). From direct current observations in the southern passages to the Caribbean Sea, Wilson and Johns (1997) determined a mean transport of 9.5 Sv into the Caribbean for the entire depth of the passages to about 1000 m depth, hence comprising the Central Water layer, which contains mainly of water from the South Atlantic. The southeastward flow along the South American continent is the Guiana Undercurrent (GUC). The NEUC seems to receive its water from the nSEC as well as from the NEC via the GUC, but partial supply also is provided out of the the NBC retroflection (Schott et al., 1998, Fig. 6b). The GUC also contributes to the EUC (Schott et al., 1998).

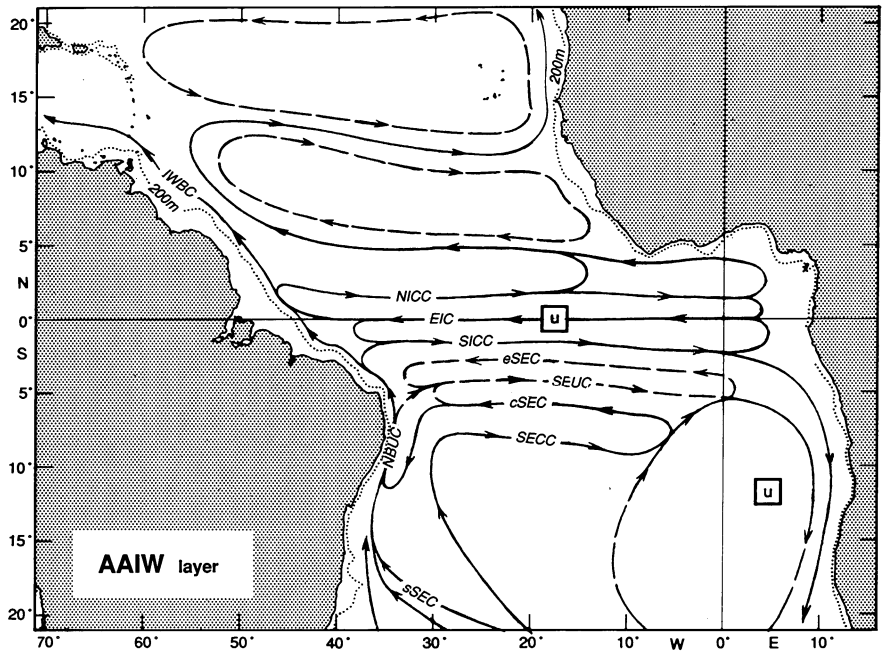

Fig. 6. Schematic map showing the horizontal distribution of the major tropical currents for the Antarctic Intermediate Water and upper Circumpolar Deep Water range at about 500–1200 m depth. Shown are the Northern Intermediate Countercurrent (NICC), the Intermediate Western Boundary Current (IWBC), the Equatorial Intermediate Current (EIC), the Southern Intermediate Countercurrent (SICC) and the North Brazil Undercurrent (NBUC), the South Equatorial Current (SEC) with the northern (nSEC), equatorial (eSEC), central (cSEC) and southern (sSEC) branches, the South Equatorial Countercurrent (SECC) and the South Equatorial Undercurrent (SEUC). Weak, not well-resolved circulation paths are shown as dashed lines. The symbol u in a square marks possible areas of upwelling, but not the exact places.

As for the TSW, no evidence for a continuous NBC flow into the Caribbean for the SACW was observed in August 1989 (Wilson et al., 1994). In boreal summer and fall the SACW apparently detours through the eastern side of the basin via the NEUC and the lower part of the NECC and the Guinea Dome. Observations in February 1993 at 7°30′N showed an interior northward pathway east of the Mid-Atlantic Ridge and only a weak signature of the direct northward flow at the continental slope of French Guiana (Arhan et al., 1998). The overall annual mean subdivision between SACW transfer along the western coast by alongshore mean flow in March–April (Schott et al., 1998) and by NBC retroflection eddy shedding in October to January is still not determined.

The SEUC is typically observed between 3°S and 5°S. According to Tsuchiya (1986) the SEUC (which he called subsurface South Equatorial Countercurrent) is a sub-thermocline flow related to the equatorial thermostad and can be recognized clearly as a continuous eastward flow at about 5°S in the west but closer to 8°S in the east with eastward-extending tongues of low salinity, high oxygen and low phosphate. The

maximum geostrophic speeds of the SEUC at 25–28°W (relative to 1000 m) have been observed at about 150 m and range from 20 to 40 cm s^{-1} (Molinari, 1982). In the source region west of 35°W the SEUC seems to be fed by oxygen-poor water from the near-equatorial SEC flow (Schott et al., 1995). East of 35°W, oxygen-rich water from the south (Tsuchiya, 1986) is transported by the SEUC, leading to a layered structure of oxygen-rich and oxygen-poor waters in the SEUC. The oxygen-rich southern water carried by the SEUC originates not directly out of the NBUC, but from southern water transported northward with the sSEC further offshore. Reverdin et al. (1991) observed seasonal variability in the SEUC, which shows opposite amplitude at the eastern and western sides of the Atlantic; while the SEUC in the east is weakest in July to September, it was strongest in the west during that time period.

South of the Cape Verde Islands the Guinea Dome also exists in the Central Water layer, and appears on the eastern side of a thermal ridge between the NEC and the NECC. In the southern hemisphere, the Angola Gyre extends into the Central Water layer, although diminished in strength compared to the surface water layer and shifted to the south. The Angola Gyre receives water from the southward alongshore shift (Hisard et al., 1976) of the SEUC and from the southward flow out of the EUC. The Angola Gyre feeds water back into the cSEC. According to the flow field proposed by Reid (1994), part of the water of the Angola Gyre continues further southward along the African coast. Shannon and Nelson (1996) suggested that thermocline water and AAIW from the tropical Atlantic are advected near the African shelf polewards into the Benguela Current, certainly as far south as 27°S. Its northwestward return at the northern side of the sSEC closes a basin-wide cyclonic gyre to the north of the subtropical gyre.

The lower part of the EUC enters the upper part of the Central Water layer and is fed out of the NBUC/NBC. In the deeper part of the Central Water layer at the equator the flow direction reverses to westward within the upper part of the Equatorial Intermediate Current (EIC) as can be seen in the velocity distribution at the equator shown by Schott et al. (1995) and Ponte et al. (1990) (Figs. 2a and b). The EUC looses its water to the overlying layer by upwelling and to the SEC branches north and south of the equator, although not much information exists on this water exchange. In the SACW layer there are upwelling sites in the EUC, as well as in the Guinea Dome and the Angola Gyre.

At 25°W just north of the equator Tsuchiya et al. (1992) described an isolated core of low oxygen and suggested a westward flow from the low-salinity region in the eastern equatorial Atlantic by way of the northern portion of the SEC. Enhanced productivity and organic regeneration in the coastal upwelling off North Africa play a part in creating the tropical oxygen minimum in the eastern North Atlantic, but very low CFC (chloroflourocarbon) values in the thermocline south of 20°N clearly demonstrate that biological activity is not the only cause. The oxygen minimum also must be physically isolated from direct ventilation with the atmosphere. Doney and Bullister (1992) concluded that the major pathway for ventilation of the SACW in the oxygen-minimum layer involves a circuitous route along the northwestward arm of the South Atlantic subtropical gyre, followed by eastward advection in the EUC. The CFC data for the oxygen minimum suggest that the time scale of this process is of the

order of several decades. Models, however, show EUC upwelling and equatorial divergence with a return flow within the SEC (Liu et al., 1994).

In the Gulf of Guinea a westward-flowing subsurface current was observed underneath the Guinea Current (Hisard and Merle, 1980), which might represent a subsurface compensatory flow of the eastward going Guinea Current and the EUC (Mittelsteadt, 1983). Since the EUC carries cool, highly saline water, the pycnocline beneath the Guinea Current is particularly intense.

The sSEC in the Central Water layer is located farther south than in the surface layer. Part of the sSEC returns eastward in the SECC, while the larger portion reaches the Brazilian coast south of 10°S, forms the NBUC (Stramma et al., 1995), and crosses the equator after surface flow intensification near 44°W as the NBC before retroflecting into the EUC. Only a weak part of the sSEC reaching the Brazilian shelf near 20°S turns southward into the Brazil Current. Direct current observations at about 20°S and 25°S (Evans and Signorini, 1985) show a southward Brazil Current flow near the Brazilian shelf in the upper 400 m.

6. The AAIW layer

The flow field of the AAIW layer based on the observations given below is shown in Fig. 6. According to Reid (1989) the AAIW presence in the interior South Atlantic is limited to the subtropical gyre south of about 25°S and a northward flow of AAIW is found west of 20°W at 20°S, which concentrates near the Brazilian coast at about 15°S and recirculates in wide parts of the tropical South Atlantic. Tsuchiya et al. (1994) described the termination of the high-oxygen core in the AAIW layer near 21°S as the transition from the anticyclonic flow south of 21°S to the cyclonic flow north of 21°S. Even at 20°S near the Brazilian shelf the flow of AAIW is northward. Direct velocity observations near 20°S and 25°S near the Brazilian shelf (Evans and Signorini, 1985) showed northward flow below 400 m depth in the AAIW layer.

The lower oxygen north of 21°S is the consequence of the southern, westward-flowing limb of the cyclonic tropical gyre in which a large amount of AAIW is first advected eastward in the Southern Intermediate Countercurrent (SICC) and is then returning westward with the sSEC. In this tropical gyre, the AAIW oxygen is severely reduced by consumption. Although velocities in this layer are weak, tracer observations indicate a cyclonic flow in the northeastern tropical South Atlantic (Fig. 6). In some flow fields presented in the literature it was tried to separate more details, but these contours are based on a few sections, and variability as well as cruise-to-cruise processing, and accuracy differences might exist. The more contoured version of Suga and Talley (1995) proposes three cells: one cyclonic cell centered at about 7°S, another centered at about 19°S in the west and 23°S in the east, and one anticyclonic cell centered at about 13°S.

There is an isolated salinity high pressed against the African coast within the tropical gyre near 10°S, most likely caused by vertical mixing (Tsuchiya et al., 1994). From tracer measurements, Warner and Weiss (1992) reported chlorofluoromethane (CFM) concentrations in the cyclonic tropical gyre to be extremely low in the AAIW

layer between the well-ventilated subtropical gyre and an equatorial tongue of enhanced CFM values. These very low CFM concentrations in the cyclonic gyre may be due to limited exchange with waters to the south or due to upwelling wihin the gyre and is marked as upwelling in Fig. 6.

Suga and Talley (1995) described salinity and nitrate maxima and oxygen minima along 25°W near 10°S and 6–7°S associated with meridional maxima of westward speeds in the AAIW from geostrophic computations relative to 3000 dbar. Coincident minima in salinity and nitrate and maxima in oxygen (Fig. 1b) are found at 8–9°S and 5–6°S at 25°W associated with meridional maxima of eastward speeds. The eastward flows may correspond with deep expressions of the SEUC and the SECC. Observations by Molinari (1982) at 25–28°W indicated that the SEUC and SECC reach into the AAIW layer. This distribution of zonal speeds and properties are not as coincident farther east as at 25°W and could not be observed in a section at the Greenwich meridian (Suga and Talley 1995). These weak current bands are included in Fig. 6, but their pathways are still obscure. As the SEUC and the SECC are still included in Fig. 6, the impression comes up that the meridional scales of the currents tend to decrease with depth; however, these currents are weak and the stronger currents are found near the equator. From the velocity distribution at $\sigma_\Theta = 27.28$ (Schott et al., 1995) it seems that the two eastward bands at 8–9°S and 5–6°S are fed mainly with water originating in the south, although the deep SEUC also receives water from the north from a deep branch of the eSEC (Schott et al., 1998).

In the western equatorial Atlantic Schott et al. (1995) could verify the existence of the EIC from direct velocity measurements, flowing westward underneath the EUC, and two off-equatorial eastward intermediate currents, the Southern and Northern Intermediate countercurrents (SICC, NICC) at 1.5–2.0 degree latitude. Schott et al. (1995) estimate the EIC transport to -20 Sv at 35°W (Fig. 2a). There is large variability in the strength and vertical extent of the EIC, and there appears to be a negative correlation in the EUC and the EIC transports. Schott et al. (1998) obtain a mean transport of -22 ± 10 Sv for the EIC at 35°W. The EIC had a minimum value of -9.5 Sv in June of 1 yr when the EUC had its strongest transport of 43.6 Sv, leading to eastward currents at the AAIW core level, while the EIC had a maximum of -30.0 Sv in November of another year when the EUC had a low value of 19.5 Sv. The variability in vertical extent of the EIC can lead to reversing currents at a selected depth (Boebel et al., 1999). A Pegasus profile taken at the equator at 30°22′W (Ponte et al., 1990) showed two westward current bands below the EUC with cores at 370 and 690 m depth. At about 32°W the EIC in June 1991 transported -6 Sv (Fig. 2b) above 400 m depth. From a mooring line during June–September 1974 along 23°30′W (Fig. 2c) Bubnov and Egorikhin (1980) obtained a transport of -31.3 Sv for the EIC (which they called Westward Intermediate Equatorial Current). Even at a mooring on the equator at 10°W westward velocities of up to 20 cm s^{-1} were observed below 400 m depth (Düing et al., 1980). No information exists on how far east the EIC is formed. From the parameter distribution at the equator Suga and Talley (1995) speculated on a westward flow along the equator but did not have the direct observations to support this.

All the observations presented above indicate the continuous existence of the EIC. According to the Schmitz and McCartney (1993) schematic flow diagram composed from a synthesis of a variety of independent investigations reported in the literature, there is also equatorial upwelling in this layer, and Roemmich (1993) attributed a convergence of about 3 Sv to the upper part of the AAIW. According to recent inverse calculations for sections at 7°30′N and 4°30′S, the AAIW layer contributes water to the central water above as well as to the upper layer of the North Atlantic Deep Water below (H. Mercier, 1997, pers. com.). According to an investigation of the AAIW on neutral surfaces dianeutral upwelling appears in the western tropical Atlantic near Brazil (You, 1999).

Only limited information is available to estimate the intermediate countercurrents. Along the mooring line at 23°30′W (Fig. 2c) there seems to be an indication of the SICC and NICC, although presented as being connected across the equator. In a hydrographic section at 25°W Tsuchiya et al. (1992) observed an isolated core of high oxygen in the AAIW layer just south of the equator. They described relatively high oxygen between 1°S and 3°S accompanied by low salinity in a tongue with its source at the western boundary and extension nearly to the eastern boundary. Suga and Talley (1995) described salinity fronts immediately south of the equator at 35°, 25°, 17.5° and 4°W and concluded that the extrema south of the front demonstrate that the salinity front south of the equator is the northern boundary of an eastward flow, which carries younger AAIW from the western boundary at least as far east as 4°W. In an LADCP profile at 1°45′S, 2°57′E, Mercier and Arhan (pers. com., 1997) observed eastward velocities of up to 20 cm s^{-1} in the AAIW layer.

Suga and Talley (1995) showed a continuous salinity front immediately north of the equator at about 2°N reaching to 4°W which becomes less sharp toward the east. A meridional maximum of oxygen occurs on the south side of the salinity front, with concentrations decreasing toward the east. This indicates that the salinity front north of the equator is associated with another eastward flow on its southern side, which is the NICC. At 25°W north and south of the equator, Doney and Bullister (1992) found CFC concentrations in the AAIW at or below the blank levels, but higher values in the equtorial band between 3°S and 3°N, representing the younger AAIW water in the SICC, EIC, NICC flow system.

Float tracks at 800 m (Richardson and Schmitz, 1993) indicated an eastward transition in the equatorial region representing the SICC and NICC, although some floats showed reversed direction after travelling to the east. Only one of the six 800 m floats deployed along the equator stayed at the equator, but this float was ballasted deep to 1125 dbar and therefore was located below the EIC in the uppermost part of the NADW. Floats in the AAIW layer off Brazil showed a southward flow near Brazil just east of the NBUC (Boebel et al., 1999). This southward flow at about 5–10°S is in agreement with the southward flow observed in the velocity field in sections at 5 and 10°S (Stramma et al., 1995) and to the adjusted steric height at 800 db (Reid, 1989). The exact pathway of this southward flow is still to be determined.

From current meter moorings at the equator along 44°W Schott et al. (1998) have shown that the NBC mean current minimum is reached at about 500 m depth and that below, near 800 m, a secondary maximum of more than 30 cm s^{-1} occurs near

the continental shelf edge, marking the AAIW layer core and the Intermediate Western Boundary Current (IWBC). Floats deployed at 800 m depth in the IWBC near the Brazilian shelf showed a northwestward continuation off the South American continent in and towards the Caribbean. Often the floats in the IWBC looped in anticyclonic eddies which the eddies translated up the western boundary. One of the floats entered the Caribbean through the Grenada Passage (Richardson and Schmitz, 1993), showing that AAIW may indeed enter the Caribbean. This path of AAIW into the Caribbean is in agreement with the direct velocity observations of Wilson and Johns (1997) in the southern passages of a weak flow into the Caribbean. The further fate of the AAIW in the Caribbean is not resolved; it does not pass through the Florida Straits (Schmitz and Richardson, 1991) but has to exit through more southerly passages.

For the tropical North Atlantic, Reid (1994) showed an anticyclonic flow between 3°N and 15°N. Talley (1996), however, states that the tropical AAIW circulation in the North Atlantic is confusing, but appears to contain a cyclonic gyre centered at 15°N, opposite to Reid's (1994) adjusted circulation. The cyclonic flow north of the equator is included in Fig. 6 by dashed flow lines but is still in part speculative and represents only a weak flow field. The westward flow at about 4°N was confirmed at 35°W in the direct velocity observations of Schott et al. (1995). In agreement with Reid's (1994) anticyclonic flow, the AAIW with the lowest salinity along a zonal section at 7°30′N (Siedler et al., 1996) was observed at the western end of the section. Further, in a meridional section along about 25°W the salinity in the AAIW layer increased northward north of about 4°N (Tsuchiya et al., 1992).

The northward flow in the AAIW layer off Africa in the North Atlantic shown by Reid (1994) had been observed also in local studies. Near the African continent northward flow in the AAIW-layer centered at 800–900 m was observed to reach up to the Canary Islands (Mittelstaedt, 1983). The AAIW salinity minimum terminates in the North Atlantic between 20°N and 25°N with a rather ill-defined boundary where it meets the Mediterranean Water in the eastern Atlantic (Talley, 1996).

7. Summary

Although several research programs have been conducted in the tropical Atlantic over the past two decades, the knowledge on the mean circulation is still fairly limited. A contributing factor certainly is the small amount of direct current observations available in the past and the degrading accuracy of the geostrophic method near the equator. In addition, the flow field contains several reversing zonal current bands of variable strengths in the tropical regions and observations are influenced by wave processes in the equatorial belt. Temporal variability between different repeat sections in the western tropical Atlantic was found for all layers described here (Schott et al., 1998). The approach of presenting a horizontal flow field here is a simplification of the three-dimensional circulation system. Vertical upwelling of about 12 Sv (Gouriou and Reverdin, 1992) exists in the equatorial region, but as it is far from being resolved where exactly upwelling and downwelling take place. Hence, symbols are only

included to represent general areas of presumed upwelling and no transport numbers are added to the schematic figures.

In this paper an attempt has been made to combine different new observations and published results to derive a schematic flow field for the tropical surface water layer, the Central Water layer, and the AAIW layer. The combination of the different findings in the literature with new observations leads to a more complete view of the tropical circulation, e.g., that the EIC, the SICC (Arhan pers.com., 1997) and the NICC extend zonally across the entire equatorial Atlantic. Of course, there are large regions where the schematic figures are highly speculative, where the exchanges and interactions between the current branches are still obscure, and other exchange routes between the currents might exist. The flow directions might change within a water mass (Fig. 2a) and the flow field is further influenced by variability (Schott et al., 1998). Hence, the flow field schematics are only meant to represent the dominating components of the circulation.

8. Appendix. List of acronyms used

Atmospheric:

ITCZ	Intertropical Convergence Zone

Water masses:

AAIW	Antarctic Intermediate Water
NACW	North Atlantic Central Water
SACW	South Atlantic Central Water
TSW	Tropical Surface Water
uCDW	upper Circumpolar Deep Water

Currents:

EIC	Equatorial Intermediate Current
EUC	Equatorial Undercurrent
GCUC	Gabon-Congo Undercurrent
GUC	Guiana Undercurrent
IWBC	Intermediate Western Boundary Current
NBC	North Brazil Current
NBUC	North Brazil Undercurrent
NEC	North Equatorial Current
NECC	North Equatorial Countercurrent
NEUC	North Equatorial Undercurrent
NICC	Northern Intermediate Countercurrent
SEC	South Equatorial Current
cSEC	central branch of SEC
eSEC	equatorial branch of SEC
nSEC	northern branch of SEC
sSEC	southern branch of SEC

SECC South Equatorial Countercurrent
SEUC South Equatorial Undercurrent
SICC Southern Intermediate Countercurrent

Acknowledgements

The field work in the western tropical Atlantic has been supported by the Bundesministerium für Wissenschaft, Forschung and Technologie, Bonn, Germany and the RV METEOR cruises by the Deutsche Forschungsgemeinschaft (DFG). One author (L.S.) started his scientific career as student of G. Siedler and thanks him for his introduction and arousing the interest to the understanding and interpretation of large scale oceanographic features. L. Talley kindly made the RV Oceanus and RV Melville data at 25°W available to us.

References

Arhan, M., Mercier, H., Bourles, B., Gouriou, Y., 1998. Hydrographic sections across the Atlantic at 7°30 N and 4°30 S. Deep-Sea Research 45, 829–872.

Boebel, O., Schmid, C., Zenk, W., 1999. Kinematic elements of Antarctic Intermediate Water in the western South Atlantic. Deep Sea Research II 46, 355–392.

Bubnov, V.A., Egorikhin, V.D., 1980. Study of water circulation in the tropical Atlantic. Deep Sea Research Part A, 26 (Suppl. II), 125–136.

Cane, M.A., 1979. The response of an equatorial ocean to simple wind stress pattern: II Numerical results. Journal of Marine Research 37, 253–299.

Defant, A., 1936. Schichtung und Zirkulation des Atlantischen Ozeans. Die Troposphäre. Wiss. Ergebn. Dt. Atlant. Exped. "Meteor" 1925–1927. 6, 289–411.

Didden, N., Schott, F., 1993. Eddies in the North Brazil Current retroflection region observed by Geosat altimetry. Journal of Geophysical Research 98, 20 121–20 131.

Doney, S.C., Bullister, J., 1992. A chlorofluorocarbon section in the eastern North Atlantic. Deep-Sea Research 39, 1857–1883.

Düing, W., Ostapoff, F., Merle, J., 1980. Physical Oceanography of the Tropical Atlantic During GATE. University of Miami, 117 pp.

Evans, D.L., Signorini, S.S., 1985. Vertical structure of the Brazil Current. Nature 315, 48–50.

Fu, L.-L., 1981. The general circulation and meridional heat transport of the subtropical South Atlantic determined by inverse methods. Journal of Physical Oceanography 11, 1171–1193.

Gordon, A.L., Bosley, K.T., 1991. Cyclonic gyre in the tropical South Atlantic. Deep-Sea Research 38 (Suppl.), S323–S343.

Gouriou, Y., Reverdin, G., 1992. Isopycnal and diapycnal circulation of the upper equatorial Atlantic Ocean in 1983–1984. Journal of Geophysical Research 97, 3543–3572.

Hisard, P., Citeau, J., Morlière, A., 1976. Le système des contre-courants équatoriaux subsuperficiels, permanence et extension de la branche sud dans l'océan atlantique. Cahier O.R.S.T.O.M., Série. Océanographic 14, 209–220.

Hisard, P., Merle, J., 1980. Onset of summer surface cooling in the Gulf of Guinea during GATE. Deep-Sea Research 26 (Suppl. II), 325–341.

Houghton, R.W., Tourre, Y.M., 1992. Characteristics of low-frequency sea surface temperature fluctuations in the tropical Atlantic. Journal of Climate 5, 765–771.

Huang, B., Shukla, J., 1997. Characteristics of the interannual and decadal variability in a general circulation model of the tropical Atlantic Ocean. Journal of Physical Oceanography 27, 1693–1712.

Lambert, R.B., Sturges, W., 1977. A thermohaline staircase and vertical mixing in the thermocline. Deep-Sea Research 24, 211–222.

Liu, Z., Philander, S.H.G., Pacanowski, R.C., 1994. A GCM study of tropical-subtropical upper-ocean water exchange. Journal of Physical Oceanography 24, 2606–2623.

Lozier, M.S., Owens, W.B., Curry, R.G., 1995. The climatology of the North Atlantic. Progress in Oceanography 36, 1–44.

Mazeika, P.A.. 1967. Thermal domes in the eastern tropical Atlantic Ocean. Limnology and Oceanography 12, 537–539.

Mittelstaedt, E., 1983. The upwelling area off Northwest Africa—a description of phenomena related to coastal upwelling. Progress in Oceanography 12, 307–331.

Molinari, R.L., 1982. Observations of eastward currents in the tropical South Atlantic Ocean: 1978–1980. Journal of Geophysical Research 87, 9707–9714.

Molinari, R.L., Garzoli, S.L., Katz, E.J., Harrison, D.E., Richardson, P.L., Reverdin, G., 1986. A synthesis of the First GARP Global Experiment (FGGE) in the equatorial Atlantic Ocean. Progress in Oceanography 16, 91–112.

Peterson R.G., Stramma, L., 1991. Upper-level circulation in the South Atlantic Ocean. Progress in Oceanography 26, 1–73.

Ponte, R.M., Luyten, J., Richardson, P.L., 1990. Equatorial deep jets in the Atlantic Ocean. Deep-Sea Research 37, 711–713.

Reid, J.L., 1989. On the total geostrophic circulation of the South Atlantic Ocean: flow patterns, tracers and transports. Progress in Oceanography 23, 149–244.

Reid, J., 1994. On the total geostrophic circulation of the North Atlantic Ocean: Flow patterns, tracers and transports. Progress in Oceanography 33, 1–92.

Reverdin, G., Rual, P., du Penhoat, Y., Gouriou, Y., 1991. Vertical structure of the seasonal cycle in the central equatorial Atlantic Ocean: XBT sections from 1980 to 1988. Journal of Physical Oceanography 21, 277–291.

Richardson, P.L., Schmitz, Jr., W.J., 1993. Deep cross-equatorial flow in the Atlantic measured with SOFAR floats. Journal of Geophysical Research 98, 8371–8387.

Richardson, P.L., Walsh, D., 1986. Mapping climatological seasonal variations of surface currents in the tropical Atlantic using ship drift data. Journal of Geophysical Research 91, 10537–10550.

Roemmich, D.H., 1983. The balance of geostrophic and Ekman transports in the tropical Atlantic Ocean. Journal of Physical Oceanography 13, 1534–1539.

Schmitz, Jr., W.J., McCartney, M.S., 1993. On the North Atlantic circulation. Reviews of Geophysics 31, 29–49.

Schmitz, Jr., W.J., Richardson, P.L., 1991. On the sources of the Florida Current. Deep-Sea Research 38 (Suppl. 1), S389–S409.

Schott, F.A., Stramma, L., Fischer, J., 1995. The warm water inflow into the western tropical Atlantic boundary regime, spring 1994. Journal of Geophysical Research 100, 24745–24760.

Schott, F., Molinari, R.L., 1996. The western boundary circulation of the subtropical Warmwatersphere. In Krauss, W. (Ed.), The Warmwatersphere of the North Atlantic Ocean, Gebr. Borntraeger, Berlin, Stuttgart, pp. 229–252.

Schott, F.A., Fischer, J., Stramma, L., 1998. Transports and pathsways of the upper-layer circulation in the western tropical Atlantic. Journal of Physical Oceanography 28, 1904–1928.

Servain, J., 1991. Simple climatic indices for the tropical Atlantic Ocean and some applications. Journal of Geophysical Research 96, 15137–15146.

Shannon, L.V., Nelson, G., 1996. The Benguela: large scale features and processes and system variability. In Wefer, G., Berger, W.H., Siedler, G., Webb, D.J. (Eds.), The South Atlantic – Present and Past Circulation. Springer, Berlin, pp. 163–210.

Siedler, G., Müller, T.G., Onken, R., Arhan, M., Mercier, H., King, B.A., Saunders, P.M., 1996. The zonal WOCE sections in the South Atlantic. In: Wefer, G., Berger, W.H., Siedler, G., Webb, D.J. (Eds.), The South Atlantic – Present and Past Circulation, Springer, Berlin, pp. 83–104.

Siedler, G., Onken, R., 1996. Eastern recirculation. In: Krauss, W. (Ed.), The Warmwatersphere of the North Atlantic Ocean. Gebr. Borntraeger, Berlin, Stuttgart, pp. 339–364.

Siedler, G., Zangenberg, N., Onken, R., Morliere, A., 1992. Seasonal changes in the tropical Atlantic circulation: Observations and simulations of the Guinea Dome. Journal of Geophysical Research 97, 703–715.

Sprintall, J., Tomczak, M., 1992. Evidence of the barrier layer in the surface layer of the tropics. Journal of Geophysical Research 97, 7305–7316.

Sprintall, J., Tomczak, M., 1993. On the formation of central water in the southern hemisphere. Deep-Sea Research 40, 827–848.

Stramma, L., 1991. Geostrophic transport of the South Equatorial Current in the Atlantic. Journal of Marine Research 49, 281–294.

Stramma, L., Fischer, J., Reppin, J., 1995. The North Brazil Undercurrent. Deep-Sea Research 42, 773–795.

Stramma, L., Schott, F., 1996. Western equatorial circulation and interhemispheric exchange. In: Krauss, W. (Ed.), The Warmwatersphere of the North Atlantic Ocean. Gebr. Borntraeger, Berlin, Stuttgart, pp. 195–227.

Stramma, L., Siedler, G., 1988. Seasonal changes in the North Atlantic Subtropical gyre. Journal of Geophysical Research 93, 8111–8118.

Suga, T., Talley, L.D., 1995. Antarctic intermediate water circulation in the tropical and subtropical South Atlantic. Journal of Geophysical Research 100, 13441–13453.

Sverdrup, H.U., Johnson, M.W., Fleming, R.H., 1942. The Oceans. Their Physics, Chemistry, and General Biology. Prentice-Hall, Englewood Cliffs, NJ, 1087 pp.

Talley, L.D., 1996. Antarctic intermediate water in the South Atlantic. In: Wefer, G., Berger, W.H., Siedler, G., Webb, D.J. (Eds.), The South Atlantic – Present and Past Circulation, Springer, Berlin, pp. 219–238.

Tomczak, M., 1984. Ausbreitung und Vermischung der Zentralwassermassen in den Tropengebieten der Ozeane. 1: Atlantischer Ozean. Oceanologica Acta 7, 145–158.

Tomczak, M., Godfrey, J.S., 1994. Regional Oceanography: An Introduction. Elsevier, Oxford, 422 pp.

Tsuchiya, M., 1986. Thermostads and circulation in the upper layer of the Atlantic Ocean. Progress in Oceanography 16, 235–267.

Tsuchiya, M., 1989. Circulation of the Antarctic intermediate water in the North Atlantic Ocean. Journal of Marine Research 47, 747–755.

Tsuchiya, M., Talley, L.D., McCartney, M.S., 1992. An eastern Atlantic section from Iceland southward across the equator. Deep-Sea Research 39, 1885–1917.

Tsuchiya, M., Talley, L.D., McCartney, M.S., 1994. Water-mass distributions in the western South Atlantic; A section from South Georgia Island (54S) northward across the equator. Journal of Marine Research 52, 55–81.

Voituriez, B., 1981. Les sous-courants équatoriaux nord et sud et la formation des dômes thermiques tropicaux. Oceanologica Acta 4, 497–505.

Wacongne, S., Piton, B., 1992. The near surface circulation in the northeastern corner of the South Atlantic Ocean. Deep-Sea Research 39, 1273–1298.

Warner, M.J., Weiss, R.F., 1992. Chlorofluoromethanes in South Atlantic Antarctic Intermediate Water. Deep-Sea Research 39, 2053–2075.

Wilson, W.D., Johns, E., Molinari, R.L., 1994. Upper layer circulation in the western tropical North Atlantic Ocean during August 1989. Journal of Geophysical Research 99, 22513–22523.

Wilson, W.D., Johns, W.E., 1997. Velocity structure and transport in the Windward Island Passages. Deep-Sea Research I 44, 487–520.

Wunsch, C., 1984. An estimate of the upwelling rate in the equatorial Atlantic based on the distribution of bomb radiocarbon and quasi-geostrophic dynamics. Journal of Geophysical Research 89, 7971–7978.

Wüst, G., 1935. Schichtung und Zirkulation des Atlantischen Ozeans. Die Stratosphäre des Atlantischen Ozeans. Wiss. Ergebn. Dt. Atlant. Exped. "Meteor" 1925–1927. 6, 109–288.

You, Y., 1999. Dianeutral mixing, transformation and transport of Antarctic Intermediate Water in the South Atlantic Ocean. Deep-Sea Research II 46, 393–435.

Zebiak, S.E., 1993. Air–sea interaction in the equatorial Atlantic region. Journal of Climate 6, 1567–1586.